

## Application of Onboard Dust Removal Technology in Fully-Mechanized Mining Face with Ultrahigh Mining Height: An Example from Bulianta Coal Mine

Xue'an Zhuang, Jinming Mo\*, Wei Ma

China Coal Technology and Engineering Group, Chongqing Research Institute, Chongqing, 400037, China

\*Corresponding Author: Jinming Mo

### ***Abstract:***

With the development of large-scale coal mining equipment, fully-mechanized mining faces with 8 m or higher mining height have been applied successfully. However, the increase in yield and mining space makes it difficult for traditional dust prevention techniques to handle dust pollution issues. In order to solve this problem, a method of dust removal by ventilation was creatively proposed for fully-mechanized mining faces. Also, exemplified by the 12513 fully-mechanized mining face of Bulianta Coal Mine, a numerical calculation model was established. By combining theory, numerical simulation and field test, an “onboard dust removal” technology was proposed and a dust collector mounted on the coal cutter was developed. Besides, with numerical simulation and industrial field experiment, it was validated that the proposed technology could reduce the dust particle mass concentration near the sidewalk by 77.2% with a comprehensive average dust suppression efficiency of 74.25%. It provides a practical basis for creating a green and safe production environment in coal mines.

***Keywords:*** Fully-mechanized mining face with high mining height, Numerical simulation, Dust removal by ventilation, Onboard dust collector, Dust pollution.

---

### I. INTRODUCTION

China has been acknowledged as the largest producer and consumer of coal resources worldwide. As an important basic energy in China, coal is conducive to promoting the development of national economy [1,2]. According to the prediction of domestic energy structure made by related organizations, clean energies will account for a significant part in 2030 though coal will occupy 60% of energy consumption [3-5]. Huge demands in coal resources have posed strict requirements on coal mine capacity and mining rate. However, efficient coal mining may cause a series of problems, among which the most significant one is dust pollution [6,7]. Dust, as a hazard jeopardizing coal mine production, mainly induces the occupational disease of pneumoconiosis. Though coal mine production safety in China has been improved obviously now, the occupational hazard of pneumoconiosis in coal mines is still rising. Based on the statistics disclosed by National Health Commission, there were 873 thousand confirmed cases of occupational pneumoconiosis in China by late 2017, among which more than 90% were pneumoconiosis and silicosis of miners. Also, the annual increase of pneumoconiosis diagnoses in miners is approximately 15 thousand. Moreover, due to low coverage of occupational health examination and imperfect employment system, the actual cases are much more than the reported ones [8-12]. In addition, dust is the leading constraint in the development of coal mine automation and intelligent mining. Dust with high concentration seriously undermines the visibility of the working region in the mining process, which causes difficulty in collecting video surveillance data and problems of weak signals and unclear images. These may further undermine the stability of monitoring, transmission and control of automatic systems. In July 2017, State Administration of Work Safety enacted the 13th Five-Year Plan for Control of Occupational Hazards, aiming to strengthen the construction of the prevention and control system for occupational diseases in coal mines and enhance the capability of occupational health supervision. The file includes dust control in underground coal mines as one key project [13].

The fully-mechanized mining face offers a prime source of dust in underground mines. Research has proven that the mass concentration of dust particles at the drum dust source of the fully-mechanized face can reach 3000 mg/m<sup>3</sup>. In consequence, efficient preventative safety solutions must be executed so as to control the dust and prevent dust dispersion to the sidewalk space, thereby reducing pollution in the miners' working environment and mitigating threats to their health [14]. In recent years, due to its high coal productivity and working efficiency, the technology for high mining heights has been developed rapidly, which is, though, followed by an increasingly serious dust pollution at the working face.

In recent years, computational fluid dynamics (CFD) has been adopted by more and more scholars to conduct numerical simulation studies on airflow-dust two-phase flow within the coal

mine tunnel. For instance, with the fluid dynamics software, Sullivan et al.[15] simulated and analyzed the airflow field and the dust migration rule near the mine tunneling machine. Geng et al. [16] adopted the method of discrete phase model (DPM) and CFD (CFD-DPM) to numerically simulate the gas-solid two-phase flow surrounding the roadway driver in the mine and analyze the distribution of airflow rate, the vortex position and the allocation of dust concentration in the working face. Also, field test was used by them to validate the numerical simulation result. Hu et al. [17] applied CFD-DPM in the study on the airflow and dust pollution actions in coal mine tunnels with varying ventilation velocities. Also, by categorizing and discussing the roadway airflow rate, the dust movement rule was analyzed in detail. With the view of inspecting the mechanism of diffusion pollution in high-density dust under forced-exhaust ventilation on fully-mechanized excavation faces, Cheng *et al.* [18] established the CFD-DEM-based airflow-dust coupling model. By combining field test with simulation, the diffusion pollution properties of dust particles with different sizes were analyzed. With the aid of the numerical simulation software, Wang et al. [19] investigated the diffusion law of airflow, dust and gas with varying axial-to-radial flow ratios under far-pressing-near-absorption ventilation conditions, thereby obtaining the axial-to-radial flow ratio with the optimal gas controlling effect. Toraño et al. [20] utilized the CFD software to study the airflow and dust field migration in the forced-exhaust mining roadway considering the influence of time, showing that the proposed model could predict dust evolution well. Also, through accelerating the rate of ventilation and widening the range between the exhaust duct and the cross-section or the floor, dust pollution could be reduced further. Kurnia et al. [21] used the CFD software to simulate the movement behavior of dust particles in coal mines.

All the aforementioned works adopted numerical simulation methods to go into the overall airflow-dust migration distribution inside the coal mine roadway. Some other researchers have proposed corresponding dust control measures [22-24] based on the simulated results. However, dust pollution at the fully-mechanized mining face still poses a major challenge. For gaining superior dust suppression performance and create healthier working conditions for miners, the methods of dust removal by ventilation in fully-mechanized excavating faces were referenced to solve the issue of dust pollution in fully-mechanized mining faces. In this paper, by taking the 12513 fully-mechanized mining face in Bulianta Coal Mine of Shendong Coal as the research subject, the research integrated numerical simulations with underground trials to study the improvement of dust pollution in the working face by the onboard dust collector.

## II. INTRODUCTION TO BULIANTA 12513 WORKING FACE

The 12513 fully-mechanized mining face in Bulianta Coal Mine of Shendong Coal locates at the 12th coal seam of No. 5 panel. The working face has a length of 327.8m, an advancing and mining length of 3090m, an average coal thickness of 7.5 m and a maximum mining length of 8 m. The designed number of cycles is 16 a day, the daily footage is 13.84 m, and the daily coal yield is 40.8 thousand tons. The full-seam mining technique is adopted for fully-mechanized mining. Field research at the 12513 fully-mechanized mining face discovers that (1) Existing dust prevention measure for the working face was mainly spraying, which had poor effects and a limited coverage. Such kind of fully-mechanized mining face has relatively large equipment and mining space. However, for traditional external spraying with a limited range, it was difficult to reach the dust source. Besides, the Shendong coal seam has a high water content, which limited the amount of water that could be used in spraying, resulting in its poor performance. (2) There are plenty of cycles per shift for the coal cutter, and the daily footage is high. Also, coal cutting by the large-scale drum and irregular, paroxysmal spalling and caving can produce large amounts of dust particles, causing high intensity of dust near the coal cutter and a long drifting distance. All these made focused treatment at the source difficult and seriously damaged the underground working environment. The situation of dust pollution on site is shown in Fig 1. Considering the dust control state of the 12513 face, an onboard dust removal technology was proposed. By installing a dust collector at the windward end face of the coal cutter, dust particles generated by coal cutting and coal seam caving were suppressed in real time.



Fig 1. Dust pollution on site

However, the fully mechanized coal mining face and coal excavating face differ substantially in their mining technology, roadway arrangement, mining equipment and

ventilation method. Therefore, after on-the-spot investigation and coordination with field staff, the paper prescribed the overall arrangement of the dust collector in the fully mechanized mining face in Fig 2. Aforementioned dust collector had a dust inlet directly facing the floor, and an individual connecting base was welded with the coal cutter. The dust collector and the connecting base were connected with a bolt.

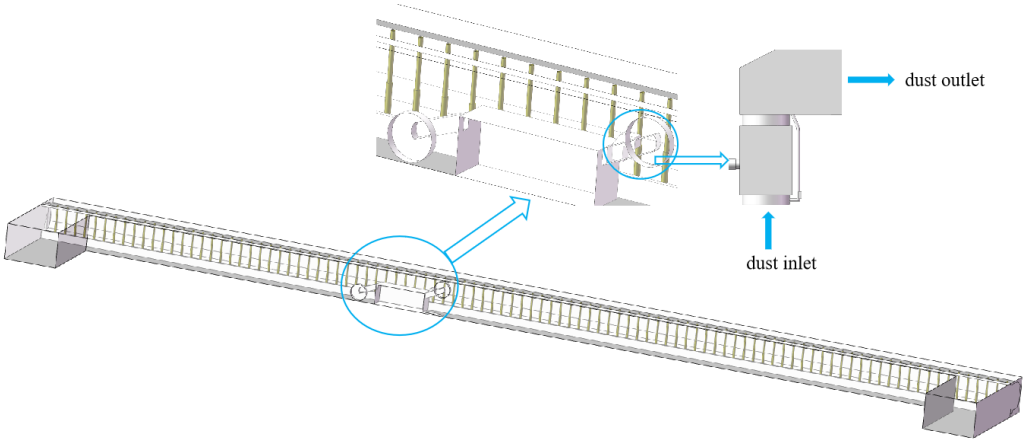


Fig 2. Schematic diagram of dust collector arrangement at fully mechanized mining face

### III. NUMERICAL SIMULATION

#### 3.1 Establishment of Physical Model

Solidworks was taken in the establishment of the three-dimensional model of the Bulianta 12513 in fully-mechanized mining face. Corresponding statistics were presented in Fig 3. The simulation mainly simulated the distribution of dust migration at the working face during coal cutting against the wind. The model was mainly consisted of the intake airway, the return airway, the coal cutter, the hydraulic support and the cable trough.

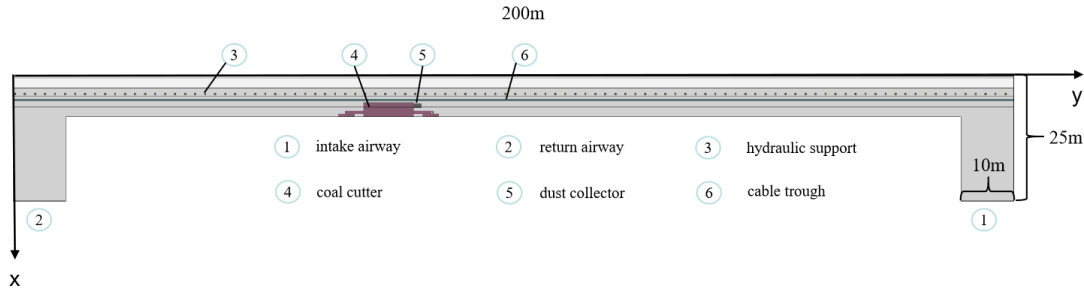


Fig 3. Three-dimensional model of fully mechanized mining face

### 3.2 Establishment of Mathematical Model

The paper adopted ANSYS-FLUENT software in the numerical simulation for airflow and dust. In view of the migration of airflow and dust, the Eulerian - Lagrangian model was illustrated in the simulated migration of airflow and the diffusion of dust. In addition, in the simulation process, the airflow was incompressible by default and regarded as continuous phase while the dust had discrete phase. Therefore, the k-ε equation was chosen to describe the migration of airflow at the fully mechanized mining face in Eulerian coordinates while the DPM in the Lagrangian coordinate system was adopted for portraying dust diffusion rule. Moreover, the interplay of airflow and dust particles and that of the particles had been taken into account [25,26].

#### (1) Mathematical model of wind flow

For the airflow of the fully mechanized coal mining face [27,28], the  $k$  equation is:

$$\frac{\partial}{\partial t}(\rho k) + \frac{\partial}{\partial x_j}(\rho k u_j) = \frac{\partial}{\partial x_j} \left[ \left( \mu + \frac{\mu_t}{\sigma_k} \right) \frac{\partial k}{\partial x_j} \right] + G_k + G_b - \rho \varepsilon - Y_M \quad (1)$$

$$G_k = \mu_t S^2, S = \sqrt{2S_{ij}S_{ij}}, S_{ij} = \frac{1}{2} \left( \frac{\partial u_j}{\partial x_i} + \frac{\partial u_i}{\partial x_j} \right)$$

The  $\varepsilon$  equation is:

$$\frac{\partial}{\partial t}(\rho \varepsilon) + \frac{\partial}{\partial x_j}(\rho \varepsilon u_j) = \frac{\partial}{\partial x_j} \left[ \left( \mu + \frac{\mu_t}{\sigma_\varepsilon} \right) \frac{\partial \varepsilon}{\partial x_j} \right] + \rho C_1 S \varepsilon - \rho C_2 \frac{\varepsilon^2}{k + \sqrt{v \varepsilon}} + C_{1\varepsilon} \frac{\varepsilon}{k} C_{3\varepsilon} G_b + S_\varepsilon \quad (2)$$

$$C_1 = \max\left(0.43, \frac{\eta}{\eta + 5}\right), \eta = S \frac{k}{\varepsilon}$$

Where  $k$  means turbulence kinetic energy ( $m^2/s^2$ );  $\rho$  indicates airflow density ( $kg \cdot m^{-3}$ );  $\mu_i$  and  $\mu_j$  are velocity components in the  $x$  and  $y$  direction ( $m \cdot s^{-1}$ ), respectively,  $\mu$  and  $\mu_t$  represent the viscosity coefficient ( $Pa \cdot s$ ) in laminar flow and turbulence, respectively;  $i, j$  are the index signs for the tensor, which can be 1, 2, or 3;  $\varepsilon$  is the diffusion rate;  $G_k$  is the turbulence kinetic energy arising from laminar velocity gradient;  $G_b$  suggests the turbulence kinetic energy induced by buoyancy;  $s_k$  and  $s_s$  are self-defined parameters;  $\gamma_m$  is the fluctuation caused by excessive diffusion, since the air was assumed to be incompressible in this work,  $\gamma_m$  was taken to be 0; while  $C_{2\varepsilon}$ ,  $C_{1\varepsilon}$ ,  $\sigma_\varepsilon$  and  $\sigma_s$  are constants in the model, which are 1.92, 1.44, 1.0 and 1.2, respectively.

## (2) Mathematical model of dust migration

From previous onsite dust concentration measurements, it was found that the volume ratio of dust particles at the fully mechanized mining face was much lower than 10% [29,30]. Therefore, the DPM model in FLUENT was employed to describe the dispersion rule of dust particles. In addition, the coupling of air and dust particles was considered in the calculation. The dust generation parameters at the fully mechanized mining face were decided according to the dust generation rule of the drum source and the caving source together with the DPM dust particle configuration. The size distribution of dust particles followed the Rosin-Rammler distribution. Besides, coal samples were collected in the field for industrial analysis by experiments, thereby determining the size distribution range of dust particles.

The trajectories of the discrete phase particles were calculated using the DPM by integrating and solving the differential equation of particle interaction in the Lagrangian coordinate system [31,32].

$$m_p \frac{du_p}{dt} = m_p \frac{\bar{u} - \bar{u}_p}{\tau_r} + m_p \frac{\bar{g}(\rho_p - \rho)}{\rho_p} + \bar{F} \quad (3)$$

where  $m_p$  means the mass of dust particles ( $mg$ ),  $\bar{u}$  denotes the fluid phase velocity ( $m/s$ ),  $\bar{u}_p$  suggests the dust particle velocity ( $m \cdot s^{-1}$ ),  $\rho$  is expressed as the fluid density ( $kg/m^3$ ),  $\rho_p$

states the density of particles ( $\text{kg/m}^3$ ),  $\vec{F}$  indicates the additional force(N),  $m_p \frac{\vec{u} - \vec{u}_p}{\tau_r}$  shows the drag force, and  $\tau_r$  is the droplet or particle relaxation time (s), [33] which can be obtained by the following formula:

$$\tau_r = \frac{\rho_p d_p^2}{18\mu} \frac{24}{C_d Re}$$

Here  $\mu$  refers to the molecular viscosity of fluid,  $d_p$  means the particle diameter,  $Re$  expresses the relative Reynolds number expressed by:

$$Re = \frac{\rho d_p |\vec{u}_p - \vec{u}|}{\mu}$$

### 3.3 Numerical simulation result of dust suppression performance for onboard dust collector at the 12513 fully mechanized mining face

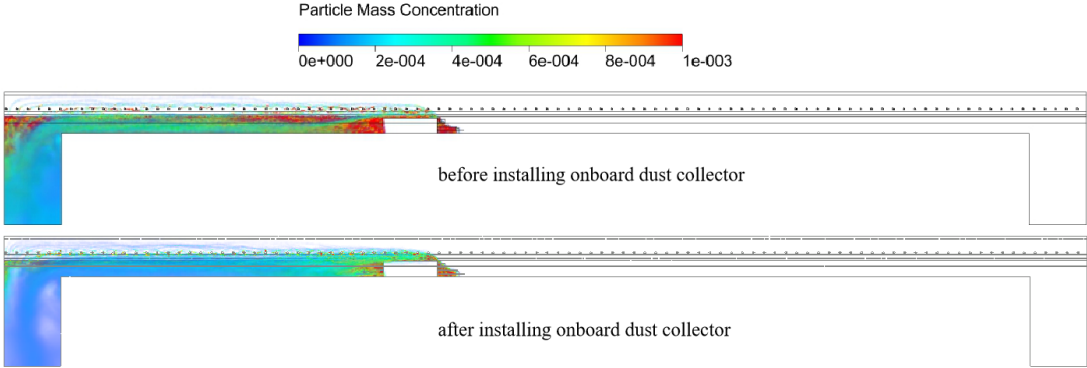


Fig 4. Influence of onboard dust collector on overall dust migration at working face

Fig 4 exhibits the allocation of overall dust migration before and after installing the onboard dust collector. It could be seen that before installation, when the dust particles moved to the coal cutter and blocked by the machine, they directly diffused to where the staff were due to lateral diffusion. The particle mass concentration was in the range of 200-650 $\text{mg/m}^3$ . Afterwards, the dust kept moving to the return airway and formed a concentrated dust zone close to the cable

trough, which was 20 m away from the front drum of the coal cutter. The dust zone had an approximate length of 30 m and a density of  $1000\text{mg/m}^3$ . In addition, there existed some high-density dust clusters at the corner of return airway. After installation, the overall dust concentration at the working face decreased significantly with a maximum particle mass concentration lower than  $750\text{mg/m}^3$ . The diffusion of dust to sidewalk was mitigated with a reduced diffusion range and a particle mass concentration lower than  $200\text{mg/m}^3$  along the diffusion path. Also, the high-density dust clusters accumulated at the return airway were relieved.

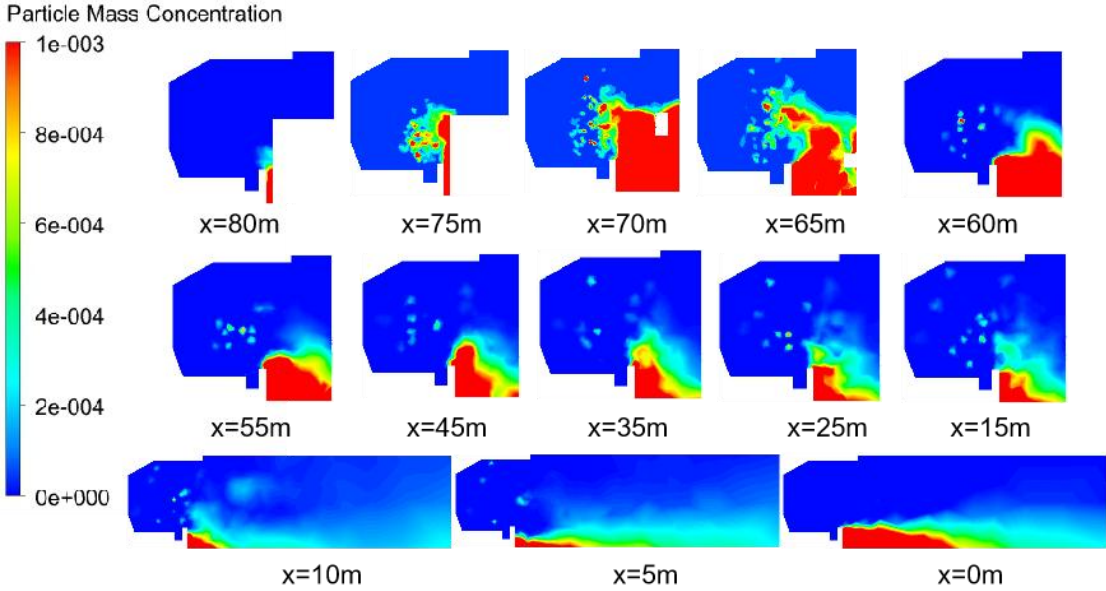


Fig 5. Distribution of dust migration at XOZ cross-section of working face before installing the onboard dust collector

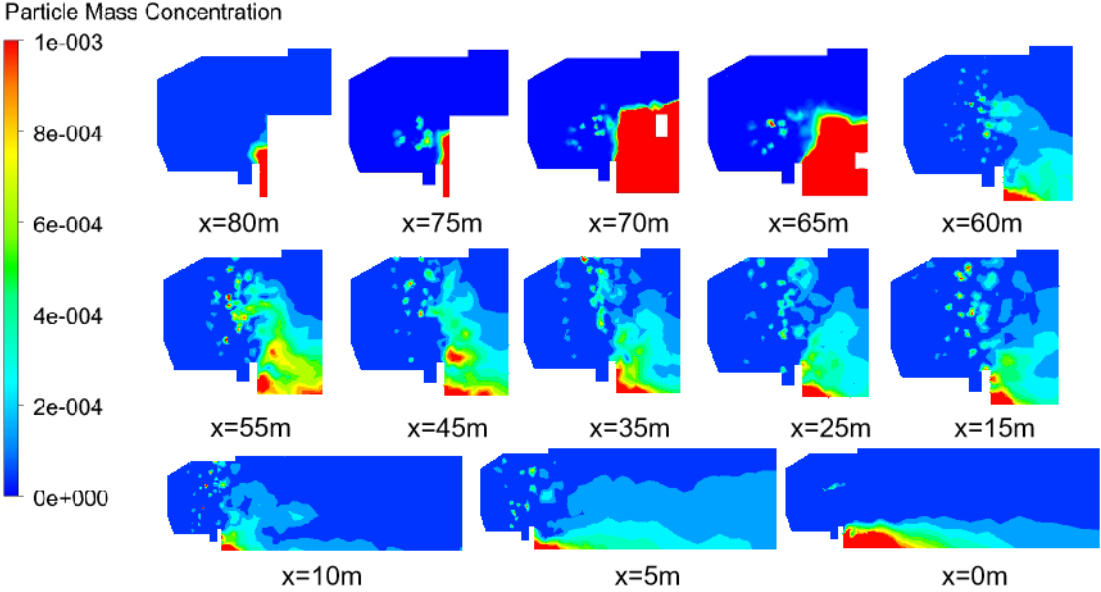


Fig 6. Distribution of dust migration at XOZ cross-section of working face after installing the onboard dust collector

Fig 5 and 6 show the distribution of dust migration at the XOZ cross-section of working face before and after installing the onboard dust collector, respectively. Thus it can be seen from Fig 5 that before installation, when the dust particles from the source moved downwind to be 5 m away from the coal cutter, they diffused to the sidewalk with a density of  $650\text{mg/m}^3$ . Possibly due to blocking of the coal cutter's end face upwind, airflow moving to this position carried the dust to diffuse sideways. Due to the extension of distance to the intake airway, the range of dust diffusion in the sidewalk region continued to increase and reached a maximum at the  $X=65\text{m}$  cross section. After that, there was little dust diffusion to the sidewalk area. Along the direction of coal mining, the dust particles focused on the coal wall side of the cable trough. By comparing with Fig 6, it could be seen that the dust pollution at the working face was alleviated after installing the onboard dust collector. Due to strong absorption of the dust collector, absorption airflow formed near the dust inlet, thereby removing most of the dust particles. Therefore, at the  $X=75\text{ m}$  cross section, merely limited dust was spread to sidewalks with maximal concentration of  $400\text{ mg/m}^3$  approximately. In  $X=70\text{ m}$  and  $X=65\text{ m}$  cross sections, the dust diffusion concentration continued to drop, though with an increasing diffusion range. In addition, comparing the cross sections of  $X=55\text{ m}$  to  $X=5\text{ m}$ , it could be seen that the overall

particle mass concentration at the working face had been decreased to a large extent after the dust collector installation, especially for the region close to the floor and the cable trough near the coal wall. However, there was an increasing trend of dust diffusion towards the roof, perhaps due to the disruption of the original airflow by the airflow of the dust outlet. Overall, the use of the onboard dust collector managed to alleviate dust pollution at the working face.

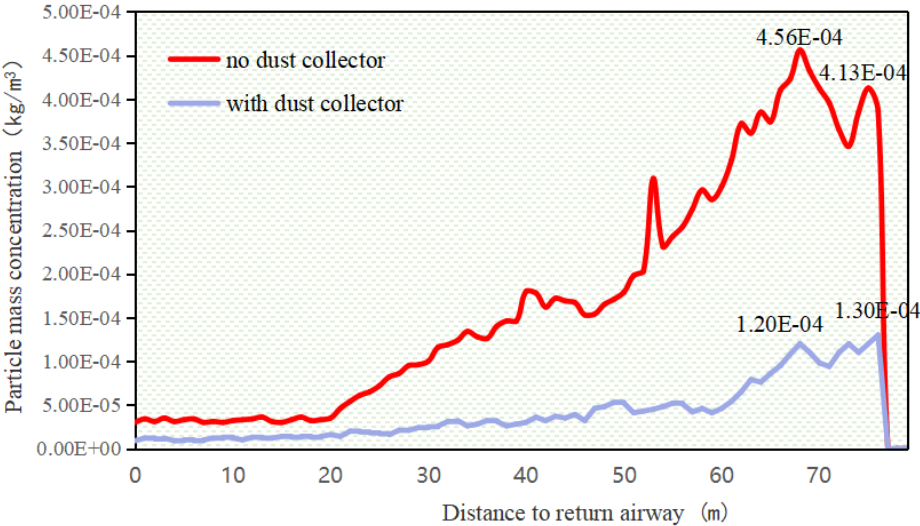


Fig 7. Dust concentration distribution along staff breathing path of the sidewalk region at the working face

The sidewalk of the working face is an area for staff activities, which should be the focus of monitoring. Fig 7 shows the dust concentration distribution along the staff breathing path of the sidewalk region downwind of the coal cutter before and after installing the onboard dust collector. It could be seen that the dust diffusion to the staff breathing zone was quite serious. Near the coal cutter driver's seat (70 m away from the return airway), maximal particle mass concentration approached 456 mg/m<sup>3</sup>. As the distance to the return airway decreased, the particle mass concentration decreased gradually. At the range of 0-20 m to the return airway, the dust concentration basically kept stable around 20mg/m<sup>3</sup>. After dust collector installation, however, the dust concentration at the staff breathing height was reduced significantly with a maximum diffusion concentration of 130mg/m<sup>3</sup>, corresponding to a maximum dust suppression efficiency of 73.68% compared to the case without the dust collector. Moreover, at a distance of 0-60 m to the return airway, the particle mass concentration was lower than 50 mg/m<sup>3</sup>. It can thus be known that the onboard dust collector makes for the improvement of dust pollution in

the working face.

### IV. ONSITE INDUSTRIAL TRIAL

For measuring onboard dust collector’s dust suppression properties and examine some possible issues during installation and use, underground experiment was conducted for the equipment, as shown in Fig 8.



Fig 8. Photo of field test for onboard dust collector

The CCZ20 respirable dust sampler was adopted and the balance weighing method was employed. The test was done when there was no hydraulic support drop column. The total particle mass concentration and dust suppression efficiency were measured both before and after installing the onboard dust collector. Two sites were tested; one was the driver’s place downwind of the coal cutter, and the other was the sidewalk region 15-20 m downwind of the coal cutter. TABLE I presents the research results as below.

**TABLE I. Dust suppression efficiency of onboard dust collector**

No.	Coal cutting process	Test site	Source	Particle mass concentration (mg/m <sup>3</sup> )	Particle mass concentration after installation (mg/m <sup>3</sup> )	Dust suppression efficiency (%)
1	Against wind	Driver's place downwind of coal cutter	Actual measurement	365	104	71.3
		15-20 m downwind of coal cutter		426	97	77.2
Driver's place downwind of coal cutter		Numerical simulation	413	130	68.5	
15-20 m downwind of coal cutter			456	120	73.7	

According to the table above, for coal cutting against the wind, the values were 365 mg/m<sup>3</sup>, 426 mg/m<sup>3</sup> and 104 mg/m<sup>3</sup>, 97 mg/m<sup>3</sup> respectively before and after dust collector installation. It could be inferred that the dust suppression efficiency 15-20 m downwind of the coal cutter was higher than that of the driver's place, and the mean of dust suppression efficacy totaled 74.25%. These measured results are similar to the numerical simulation results as shown in Fig 7, demonstrating good dust suppression effect of the onboard dust collector.

Since the installation of the onboard dust collector, the device had functioned normally for three months. Then a large piece of falling waste rock hit the top corrugated plate of the dust collector, damaging its filter section. After analysis it was known that the damage was due to insufficient strength of the maintenance window in the corrugated plate. The impact of the waste rock caused deformation in its vulnerable position. One side of the maintenance window went up and was impacted by the waste rock for several times. The maintenance window was thus damaged, resulting in damage of both the ventilation window and the corrugated plate. Field inspection found that the connection between the dust collector and the coal cutter was relatively stable with decent overall strength. However, the strength of the region should be enhanced, especially the deformation resistance at its top. In addition, to prevent equipment damage due to impact of falling waste rocks, the shell of the onboard dust collector close to the

coal wall should be made to be integral and seamless. Also, the maintenance window can be moved to the other side near the sidewalk, thereby avoiding influence from falling rocks.

## V. CONCLUSION

At the fully mechanized mining face, the caving of coal seam can generate large quantities of dust particles, causing environmental pollution. In order to solve this problem, by taking the 12513 fully mechanized mining face in Bulianta Coal Mine of Shendong Coal, a dust removal technology by ventilation was innovatively proposed in this research. By installing a dust collector on the coal cutter, the dust generated by coal cutting and coal seam caving could be handled in real time. Also, through integrating numerical simulation with field test, the dust suppression effect of the onboard dust collector was studied. Suggestions on further improvement were given as well. The following conclusions were drawn from this study.

1) When the dust particles generated by the caving coal seam moved to the coal cutter, they were blocked by the machine and diffused sideways to the activity region for staff, causing a particle mass concentration of  $200\text{-}650\text{mg/m}^3$ . With the increase of distance to the return airway, the dust diffusion range continued to increase in the sidewalk region, reaching a maximum at the  $X=65\text{m}$  cross section. In addition, around 20 m away from the front drum of the coal cutter, a concentrated dust zone around 30 m long formed near the cable trough, the particle mass concentration of which exceeding  $1000\text{ mg/m}^3$ . Moreover, some dust clusters existed at the corner of the return airway.

2) As indicated by numerical simulation results, the application of onboard dust collector obviously improved the problem of dust pollution at the working face. The maximum dust diffusion density was lowered to be  $400\text{mg/m}^3$ , but the diffusion range was increased. In the meantime, dust diffusion to the top rose at the working face. Moreover, comparison of dust concentration in the sidewalk breathing zone for staff before and after installing the dust collector found that there was little dust diffusion after the installation.

3) As demonstrated by the industrial test of the onboard dust collector, for cutting against the wind, the dust suppression efficiencies reached 71.3% and 77.2% at the driver's place and 15-20 m downwind of the coal cutter, the comprehensive average dust suppression efficiency was 74.25% with high performance. Also, the experimental results were consistent with numerical simulation results. According to field use situation, improvement suggestions were given for the onboard dust collector.

## ACKNOWLEDGEMENTS

The program is sponsored by National Key R&D Program of China under Project No. 2017YFC0805200).

## REFERENCES

- [1] Li R., Leung G.C.K., (2012)Coal consumption and economic growth in China, *Energy Policy*. 40: 438-433.
- [2] Yang S.B., Nie W., Liu S.S., Liu Z.Q., Peng H.T., Ma X., Cai P., Xu C.W., (2018)Effects of spraying pressure and installation angle of nozzles on atomization characteristics of external spraying system at a fully-mechanized mining face, *Powder Technology*. 343: 754-764.
- [3] General Office of the State Council of the People's Republic of China, *Strategic Action Plan for Energy Development*, vols. 2014-2020, (2014): 6-7.
- [4] Ding Y.M., Ezekoye O.A., Lu S.X., Wang C.J., Zhou R., (2017) Comparative pyrolysis behaviors and reaction mechanisms of hardwood and softwood, *Energy Convers. Manag.* 132: 102-109.
- [5] Kong B., Li Z.H., Wang E.Y., Lu W., Chen L., Qi G.S., (2018) An experimental study for characterization the process of coal oxidation and spontaneous combustion by electromagnetic radiation technique, *Process Saf. Environ.* 119: 285-294.
- [6] Lu X., Zhu H., Wang D.M.,(2017) Investigation on the new design of foaming device used for dust suppression in underground coal mines.315: 270-5.
- [7] Geng F., Zhou F., Luo G.,(2014) Research status and method *Mining Safety & Environmental Protection*.41(5):5.
- [8] Ross M.H., (2019) Murray JJOM. (2004) Occupational respiratory disease in mining. 54 (5): 304-10.
- [9] Yin S., et al. Transient CFD modelling of space-time evolution of dust pollutants and air-curtain generator position during tunneling. *Journal of Cleaner Production*.
- [10] Wang H., Wang D., Tang Y., Wang Q., (2015) Foaming agent self-suction properties of a jet-type foam preparation device used in mine dust suppression, *Process. Saf. Environ.Prot.* 98: 231-238.
- [11] Li F., Zhanyou S., Wang Y., Zhang H., (2010) Study on the dust concentration distribution and migration in flat-type chamber stope based on fluent software, *Miner. Res.Dev.*

- [12] Wang Q., Wang D., Wang H., Han F., Zhu X., Tang Y., Si W., (2015) Optimization and implementation of a foam system to suppress dust in coal mine excavation face, *Process.Saf. Environ. Prot.* 96: 184-190.
- [13] SAWS. The 13th Five-year plan of occupational 2017. Ministry of Emergency Management of the People's Republic of China.
- [14] Dawei C., Wen N., Peng C., et al. (2018) The diffusion of dust in a fully-mechanized mining face with a mining height of 7 m and the application of wet dust-collecting nets. *Journal of Cleaner Production*, S0959652618327215-.
- [15] Sullivan P., Heerden JV., (1993) Simulation of environmental conditions in continuous miner developments using computational fluid dynamics. *Journal of the Mine Ventilation Society of South Africa*, 46 (1): 2-11.
- [16] Hu S.Y., Liao Q., Feng G.R, Huang Y.S., Shao H., Fan Y.R., Ye Y.B.(2019) Numerical study of gas-solid two-phase flow around road-header drivers in a fully mechanized excavation face, *Powder Technology*.344:959-969.
- [17] Hu S., Liao Q., Feng G., Huang Y., Shao H., Gao Y., Hu F., (2020) Influences of ventilation velocity on dust dispersion in coal roadways, *Powder Technology*. 360: 683-694.
- [18] Yu H., Cheng W., Wu L., et al. (2017) Mechanisms of dust diffuse pollution under forced-exhaust ventilation in fully-mechanized excavation faces by CFD-DEM. *Powder Technology*. 317: 31-47.
- [19] Li Y., Wang P.F, Liu R.H, Jiang Y.D, Han H., (2019) Determination of the optimal axial-to-radial flow ratio of the wall-mounted swirling ventilation in fully mechanized excavation face, *Powder Technology*.
- [20] Toraño, Torno S., Menéndez M., Gent M., (2011) Auxiliary ventilation in mining roadways driven with roadheaders: Validated CFD modelling of dust behavior, *Tunnelling & Underground Space Technology*. 26: 201-210.
- [21] Kurnia J.C., Sasmito A.P., Hassani F.P., Mujumdar A.S., (2015) Introduction and evaluation of a novel hybrid brattice for improved dust control in underground mining faces: a computational study, *International Journal of Mining Science and Technology*. 25: 537-543.
- [22] Zhou G., Zhang Q., Bai R.N., Fan T., Wang G. (2017) The diffusion behavior law of respirable dust at fully mechanized caving face in coal mine: CFD numerical simulation and engineering application, *Process Safety and Environmental Protection*. 106: 117-128.
- [23] Ren T., Wang Z.W., Zhang J., (2018) Improved dust management at a longwall top coal caving (LTCC) face - A CFD modelling approach, *Advanced Powder Technology*. 29: 2368-2379.

- [24] Dawei C., Wen N., Peng C., et al. (2018) The diffusion of dust in a fully-mechanized mining face with a mining height of 7 m and the application of wet dust-collecting nets. *Journal of Cleaner Production*, S0959652618327215-.
- [25] Gang Z., Bo F., Wenjing Y., et al. (2018) Numerical simulations on airflow-dust diffusion rules with the use of coal cutter dust removal fans and related engineering applications in a fully-mechanized coal mining face. *Powder Technology*, S003259101830576X-.
- [26] Liu Q., Nie W., Hua Y., et al. (2018) The effects of the installation position of a multi-radial swirling air-curtain generator on dust diffusion and pollution rules in a fully-mechanized excavation face: A case study. *Powder Technology*. 329.
- [27] Chang P., Xu G., Zhou F.B., Mullins B., S. Abishek, (2019) Comparison of underground mine DPM simulation using 651 discrete phase and continuous phase models, *Process Saf. Environ. Prot.* 127: 45-55.
- [28] Hu S.Y., Feng G.R., Ren X.Y., Xu G., Chang P., Wang Z., Zhang Y.T., Li Z., Gao Q., (2016) Numerical study of gas-solid 655 two-phase flow in a coal roadway after blasting, *Adv. Powder Technol.* 27: 1607-1617.
- [29] Wang P.F., Tian C., Liu R.H., Wang J., (2019) Mathematical model for multivariate nonlinear prediction of SMD of X-type swirl pressure nozzles, *Process Saf. Environ. Prot.* 125: 228-237.
- [30] Wang Y.P., Jiang Z.A., Chen J.S., Chen J.H., Wang M., (2019) Study of high-pressure air curtain and combined dedusting of gas water spray in multilevel ore pass based on CFD-DEM, *Adv. Powder Technol.* 30: 1789-1804.
- [31] Zhou G., Feng B., Yin W.J., Wang J.Y., (2018) Numerical simulations on airflow-dust diffusion rules with the use of coal cutter dust removal fans and related engineering applications in a fully-mechanized coal mining face, *Powder Technol.* 339: 354-367.
- [32] Li Y.J., Wang P.F., Liu R.H., Gao R.Z., (2019) Optimization of structural parameters and installation position of the wall-mounted air cylinder in the fully mechanized excavation face based on CFD and orthogonal design, *Process Saf. Environ. Prot.* 130: 344-358.
- [33] Xu C.W., Nie W., Liu Z.Q., Peng H.T., Yang S.B., Q. Liu, (2019) Multi-factor numerical simulation study on spray dust suppression device in coal mining process, *Energy*. 182: 544-558.